Title
Exploring Metabolism In Vivo Using Endogenous 11C Metabolic Tracers

Journal
Seminars in Nuclear Medicine, 47(5)

ISSN
0001-2998

Authors
Neumann, Kiel
Flavell, Robert
Wilson, David M

Publication Date
2017-09-01

DOI
10.1053/j.semnuclmed.2017.05.003

Peer reviewed

HHS Public Access

Author manuscript

Semin Nucl Med. Author manuscript; available in PMC 2018 July 09.

Published in final edited form as:

Semin Nucl Med. 2017 September ; 47(5): 461–473. doi:10.1053/j.semnuclmed.2017.05.003.

Exploring metabolism *in vivo* using endogenous ^{11}C metabolic tracers

Kiel Neumann[1], **Robert Flavell**[1], and **David M. Wilson**[1,*]

[1]Department of Radiology and Biomedical Imaging, University of California, San Francisco, San Francisco, CA 94158, USA

Abstract

Cancer and other diseases are increasingly understood in terms of their metabolic disturbances. This thinking has revolutionized the field of *ex vivo* metabolomics and motivated new approaches to detect metabolites in living systems including proton magnetic resonance spectroscopy (^{1}H-MRS), hyperpolarized ^{13}C MRS, and positron emission tomography (PET). For PET, imaging abnormal metabolism *in vivo* is hardly new. Positron-labeled small-molecule metabolites have been used for decades in humans, including ^{18}F-FDG, which is used frequently to detect upregulated glycolysis in tumors. Many current ^{18}F metabolic tracers including ^{18}F-FDG have evolved from their ^{11}C counterparts, chemically identical to endogenous substrates and thus approximating intrinsic biochemical pathways. This mimicry has stimulated the development of new radiochemical methods to incorporate ^{11}C and inspired the synthesis of a large number of ^{11}C endogenous radiotracers. This is in spite of the 20-minute half-life of ^{11}C, which generally limits its use in patients to centers with an on-site cyclotron. Innovation in ^{11}C chemistry has persisted in the face of this limitation, because (1) the radiochemists involved are inspired (2) the methods of ^{11}C incorporation are diverse and (3) ^{11}C compounds often show more predictable *in vivo* behavior, thus representing an important first step in the validation of new tracer concepts. In this mini-review we will discuss some of the general motivations behind PET tracers, rationales for the use of ^{11}C, and some of the special challenges encountered in the synthesis of ^{11}C endogenous compounds. Most importantly, we will try to highlight the exceptional creativity employed in early ^{11}C tracer syntheses, which used enzyme-catalyzed and other “green” methods before these concepts were commonplace.

Introduction

The study of endogenous radiotracers holds special appeal in nuclear medicine. Of the positron-emitting nuclei (^{15}O, ^{13}N, ^{11}C) corresponding to atoms commonly found in endogenous metabolites, ^{11}C is the most versatile and best-studied, with a half-life (20 minutes) allowing its incorporation into many small-molecules of biologic interest. As this review will describe, numerous endogenous ^{11}C positron emission tomography (PET) radiotracers have been reported, including sugars, amino acids, nucleosides, and antioxidants. Since these are chemically and biochemically identical to their ^{12}C

*Corresponding Author: David Wilson, M.D., Ph.D., Department of Radiology and Biomedical Imaging, University of California, San Francisco, 505 Parnassus Ave., San Francisco, CA 94143, Phone: (415) 353-1668, Fax: (415) 353-8593, david.m.wilson@ucsf.edu.

counterparts, in many respects they offer the purest study of human metabolism. Increasingly, numerous highly prevalent diseases are understood in terms of their metabolic derangements, including cancer, diabetes, and fatty liver disease. Recent developments in the understanding of these diseases have led to a resurgence of interest in metabolomics, studied both *ex vivo* and in living systems. Several imaging techniques are well-suited to this analysis, including ^{1}H magnetic resonance spectroscopy (MRS), hyperpolarized ^{13}C MR spectroscopy, and PET.

The success of ^{18}F-FDG in the study of human cancers highlights the power of metabolic technologies in understanding and treating human disease. In the case of ^{18}F-FDG, the target is highly glycolytic cells, that upregulate glucose (GLUT) transporters as well as hexokinase, thus trapping the phosphorylated ^{18}F-FDG adduct intracellularly. This simple mechanism is the basis for cancer detection, staging, and treatment evaluation in several clinical scenarios. However, as any radiochemist will appreciate ^{18}F-functionalized metabolites frequently do not perform as intended. Since endogenous molecules do not contain fluorine, ^{18}F tracers are not sterically, chemically, or biochemically equivalent to their unmodified counterparts. As we will highlight comparing PET versions of Vitamin C, ^{18}F substitution can markedly alter the transport properties of the molecule. Furthermore, unintended reactions *in vivo* in particular ^{18}F defluorination can significantly confound interpretation of imaging data. In the context of these obstacles, radiosynthesis of the endogenous ^{11}C species may be worth the additional expense and difficulty- providing a starting point for modification with longer half-life nuclei.

In this review, we will summarize the basic approaches used in PET to identify tumors and other abnormalities, including affinity-based, microenvironment-responsive, and metabolic strategies. The primary role of endogenous ^{11}C radiotracers is in this final category, whereby the mechanism of contrast depends on host metabolism of the positron-emitting substrate. We will survey the basic methods employed to generate ^{11}C endogenous tracers, several of which have used living systems. For example, an early synthesis of ^{11}C glucose relied on the metabolism of ^{11}C CO_2 during photosynthesis. Increasingly, the ingenuity of radiochemistry labs has allowed chemical synthesis of ^{11}C endogenous molecules from simple building-blocks, including ^{11}C methyl-iodide and ^{11}C cyanide. We will also discuss special challenges faced in the synthesis of endogenous ^{11}C radiotracers, including the development of enantomerically-pure ^{11}C amino acids, and unintended incorporation of carrier into the target molecule. Finally, we will survey the success stories in this field, whereby ^{11}C endogenous tracers have been used to interrogate basic biochemistry. As interest in metabolism expands and evolves, PET will be used in conjunction with other metabolic technologies to explore the chemistry of living systems.

PET tracers- general strategies

From a clinical perspective, PET is already a highly useful technology with the potential for application to numerous new disease targets. Whereas the most common techniques used in clinical imaging, computed tomography (CT) and magnetic resonance imaging (MRI) largely provide anatomic information, PET is employed to investigate function, based on the biodistribution of a positron-emitting nucleus in the body. Positron-emitting nuclei include

^{11}C and ^{18}F, which are appealing based on their relatively long half-lives (20 minutes for ^{11}C and 120 minutes for ^{18}F), and minimal perturbations of known drug or metabolite structures. For the purposes of this review, we will limit our discussion to these nuclei, although remarkable progress has been made in recent years using other nuclei (eg. ^{68}Ga), which can also be incorporated into targeted small molecules via chelating groups(1–4). In a typical clinical PET study, a radiotracer labeled with one of these nuclei is administered intravenously to a patient. Following a delay, images of the patient are acquired via a PET scanner, which is frequently incorporated into a dual-modality instrument, PET-CT or PET-MRI for simultaneous acquisition of functional and anatomic information.

The specific mechanisms of PET tracer uptake and retention are increasingly investigated more rigorously, in cancer and other diseases. In general, these mechanisms require both disease-specific retention of the PET tracer, and elimination of nonspecific activity or “background.” There are three basic PET tracer strategies: (1) affinity based (2) microenvironment-sensitive and (3) metabolic, whereby retention of the tracer depends on metabolism by host machinery. PET tracers using these divergent strategies can be used to study the same disease. For example, the metabolic probe ^{18}F-FDG has been used to identify the characteristic pattern of hypometabolism in Alzheimer’s disease, to complement the application of affinity-based amyloid and tau tracers.

Affinity-based PET probes represent a very large number of published tracers. In many cases, the starting point is known pharmacology for a given receptor-ligand pair. Incorporation of the PET nucleus is often performed to minimize steric or electronic perturbations, so as to retain high-affinity binding. Recent examples of high-affinity PET tracers include those developed for neurodegenerative disease, in particular targeting amyloid plaques and tau-derived neurofibrillary tangles(5–8). The development of high-affinity PET tracers for beta-amyloid highlights a fairly typical progression for affinity-based probes. An early, major accomplishment in this area was the development of Pittsburgh compound B, ^{11}C PiB whose structure was derived from thioflavin T, a dye used for histologic staining of misfolded protein aggregates(9). The chemical structure of ^{11}C PiB as well as an early ^{11}C PiB PET scan in an Alzheimer’s patient are shown in Figure 1. Since the use of short half-life ^{11}C tracers is largely restricted to large medical centers with an on-site cyclotron, subsequent efforts focused on the development of high performance ^{18}F tracers including ^{18}F-florbetapir (^{18}F-AV-45)(10). Currently, ^{18}F-AV-45 is commercially available (Siemens), allowing use at centers without a cyclotron or radiopharmaceutical facility. The success of affinity-based methods is further highlighted by the success of recent approaches targeting prostate-specific membrane antigen (PSMA), which is highly expressed in a number of prostate cancers. Two approaches show high promise, including a phosphoramidate-derived tracer which uses substrate mimicry to yield a high affinity ^{18}F ligand(11). Another successful ligand is ^{68}Ga-PSMA, which takes advantage of low-cost ^{68}Ga generators to yield a method that has shown early promise in the detection and management of prostate cancer. In general, affinity-based PET tracers require a very low dissociation constant (K_d) in the nM or pM range and include both small-molecules and antibodies. Careful consideration to specific activity is also essential to affinity-based strategies.

A second strategy uses the disease microenvironment to sequester PET nuclei. The best example is ^{18}F-fluoromisonidazole (FMISO), which undergoes chemical transformation in tissues with low oxygen tension, with multiple reductions resulting in species capable of covalent binding to macromolecules, or conjugation to reduced glutathione (GSH)(12). These transformations are shown in Figure 2, as is a FMISO scan demonstrating the effects of radiation therapy on a brain tumor(13). A large number of additional hypoxia-sensitive tracers have been reported, several of which are also imidazole-derived, but others, including ^{64}Cu-ATSM, rely on tumoral reduction of Cu(II)(14). Recently, other tumor-specific analytes have been targeted, including acid (H^+)(15), reactive oxygen species (in particular H_2O_2)(16), and formaldehyde(17). These strategies have used analyte-sensitive, metastable ^{18}F-FDG and ^{18}F-FLT precursors to show specific accumulation in cells and preclinical models with a pH-sensitive strategy shown in Figure 3.

Finally, several of the most successful PET tracers depend on biotransformation for image contrast. These tracers can either be chemically identical to an endogenous substrate (^{11}C-thymidine), or a well-tolerated mimic (thymidine analog ^{18}F-FLT). The best known metabolic PET tracer is ^{18}F-FDG, in which ^{18}F is substituted for a hydroxyl group at the 2-position. This substitution does not impede ^{18}F-FDG by GLUT transporters (primarily GLUT 1,3,4) or phosphorylation at the 6-position by hexokinase, but isomerization to fructose (glucose phosphate isomerase) is effectively blocked. Thus, trapping of ^{18}F-FDG becomes a surrogate for GLUT transporter and hexokinase expression, which are up-regulated in most cancers. Of note, the contrast obtained in a PET-FDG scan is partially related to charge trapping; the phosphorylated ^{18}F-FDG adduct is retained in the cell, as opposed to the behavior of readily diffusible, nonpolar molecules.

Beyond glycolysis-the power of metabolic strategies

The success of ^{18}F-FDG in oncology is perhaps not surprising, given that cancer is increasingly understood as a metabolic disease. A large number of metabolic pathways have been exploited for cancer diagnosis, including glycolysis, DNA synthesis, glutaminolysis, membrane synthesis, and antioxidant cycling. The role of metabolic reprogramming in cancer pathogenesis is highlighted in the discovery of numerous oncometabolites including 2-hydroxyglutarate (2-HG), that is produced in cancer-associated isocitrate dehydrogenase 1 (IDH1) mutations(18–20). Strikingly, 2-HG is not a mere bystander of abnormal metabolism- but rather itself an epigenetic modifier that influences DNA and histone demethylation. The discovery of this oncometabolite was quickly followed by reports of imaging methods used to detect it, with 2-HG successfully identified by ^{1}H-MRS using spectral editing techniques(21,22). With its power to generate structures derived from endogenous molecules, PET is well suited to interrogate the divergent metabolism seen in cancer and other diseases.

Why ^{11}C?

The PET radionuclei incorporated into endogenous molecules include ^{11}C, ^{13}N, and ^{15}O, with respective half-lives of 20 minutes, 10 minutes, and 2 minutes respectively. Of these, ^{11}C is clearly best-suited to incorporation into complex organic structures, based on the

relatively long half-life and diversity of precursor molecules available for use. Endogenous ^{11}C structures are also amenable to enzymatic and even “living” syntheses, based on their homology to natural substrates. In fact, the chemistry of ^{11}C building blocks can be simpler than that of ^{18}F precursors, providing an important starting point for evaluation of a new tracer concept.

The main justification for using ^{11}C tracers to study metabolism is their close approximation of endogenous molecules. In many cases, ^{18}F substituted structures fail to replicate the biochemical modification needed for tracer uptake and accumulation. The difference between endogenous ^{11}C molecules and their ^{18}F counterparts is highlighted by studies of ascorbate-derived PET tracers. One potential application of PET versions of Vitamin C is that they undergo ascorbate-recycling in response to reactive oxygen species, generating sensors that are potentially responsive to oxidative stress. Vitamin C undergoes a two-electron oxidation to dehydroascorbic acid (DHA), which in solution exists as both hydrated and bicyclic forms. The bicyclic version of DHA is postulated to undergo rapid GLUT transport, based on its structural similarity to glucose(23,24). The first synthesis of ^{18}F-Vitamin C was accomplished with ^{18}F incorporated at the 6-position by Kothari et al., generating a molecule incapable of forming a bicyclic species due to the substitution of ^{18}F for a hydroxyl group(25,26). Recently, a synthesis of ^{11}C Vitamin C was reported, for which the authors reported accumulation of ^{11}C in ROS-producing cells via ascorbate recycling(27). The presumed mechanism of ^{11}C ascorbate recycling is shown in Figure 4. Another study contrasted ^{11}C and ^{18}F analogs more explicitly, via the comparison of L-[β-11C] DOPA and 6-fluoro-[β-11C]-L-DOPA(28). Significant differences in brain radiotracer deposition were seen in a monkey model, suggesting that ^{11}C L-DOPA and ^{18}F L-DOPA tracers are non-identical with respect to their distribution *in vivo*.

The liveliest syntheses of endogenous ^{11}C tracers

Early development of ^{11}C tracers required considerable ingenuity, harnessing living systems, and the specificity of enzymes. For example, an early synthesis of ^{11}C glucose used photosynthesis, via exposure of Swiss chard leaves to ^{11}C-CO_2 followed by separation using liquid chromatography(29). This method is contrasted with the first direct radiochemical synthesis of ^{11}C glucose using reaction of ^{11}C-HCN with D-arabinose followed by reduction(30).

One of the main advantages of using enzymes in PET radiosynthesis is their inherent substrate specificity, particularly useful for the enantiomeric resolution of racemic mixtures. A remarkable example is the synthesis of L-aromatic amino acids, ^{11}C tyrosine and ^{11}C tryptophan(31). The starting material for their syntheses was racemic ^{11}C alanine, generated from ^{11}C HCN via a Strecker synthesis. As shown in Figure 5, alanine is converted to pyruvate by oxidation/hydrolysis (D-amino acid oxidase, glutamic-pyruvic transaminase), and to tyrosine and tryptophan by the actions of β-tyrosinase and tryptophanase, respectively. Most ingenious is the use of D-amino acid oxidase, which uses flavin adenine dinucleotide (FAD) as a cofactor to selectively oxidize the D-enantiomer, allowing separation of the ^{11}C L-amino acid from the mixture.

^{11}C building blocks for chemical synthesis

Historically, the most important technical advances in the widespread use of endogenous ^{11}C tracers were the syntheses of reactive ^{11}C building blocks (in particular ^{11}C MeI), and the development of automated/remote-controlled synthesis equipment. The building blocks most frequently used in the syntheses of ^{11}C endogenous radiotracers are summarized in Figure 6. Their use in ^{11}C tracers falls into three main categories: methylations, cyanations, and carbonyl chemistry (CO_2, CO, $COCl_2$). Several excellent reviews have highlighted methods of ^{11}C incorporation into radiopharmaceuticals(32–35).

One of the most significant advances in ^{11}C radiotracer synthesis was the development of ^{11}C MeI. Methylations using ^{11}C MeI are an excellent way to label a substrate containing a nucleophilic oxygen, nitrogen, or sulfur. One of the first PET radiotracers to use ^{11}C MeI was ^{11}C methionine, formed by the reaction between ^{11}C MeI and a homocysteine-derived precursor. The first radiosynthesis of ^{11}C L-methionine used an S-benzyl protected precursor in Na/NH_3, which allowed both facile reduction and deprotonation of the reactive thiol(36). Although this method allowed generation of ^{11}C L-methionine with very high enantiomeric excess (> 99%), it has been replaced by a convenient technique using the cyclic precursor L-homocystine-thiolactone(37). Despite the lower reported enantiomeric excess (approximately 70–80%), this is not considered critical for most imaging applications. These syntheses are shown in Figure 7.

Special synthetic challenges

A significant challenge in ^{11}C radiochemistry has been the synthesis of chiral amino acids. In some cases incorporation of ^{11}C occurs away from the key chiral center, for example in the synthesis of ^{11}C methionine or ^{11}C glutamine(38). However, in other cases ^{11}C chiral amino acid synthesis has employed methods that yield racemic mixtures, in the absence of clever chemical and biochemical strategies. Synthesis of racemic [1-^{11}C] L-alanine is most commonly performed via the Strecker synthesis, in which ^{11}C-CN is incorporated into an aldehyde analog, in this case a bisulfate adduct followed by treatment with ammonium hydroxide(39). Analogous procedures have been performed for [1-^{11}C] leucine(40) and [1-^{11}C] tyrosine(41). For synthesis/purification of the pure L-enantiomer, several methods have been employed including (1) separation using high performance liquid chromatography (HPLC) on a chiral stationary phase (2) enzymatic resolution (3) use of a chiral auxiliary, usually glycine-derived (4) application of a chiral catalyst, either for selective hydrogenation or alkylation.

Alkylation of glycine-derived structures is a frequently applied method to yield [3-^{11}C] amino acids. These have included use of [(+)-2-hydroxypinanyl-3-idene] glycine *tert*-butyl ester(42), the Schiff base of (S)-O-[*N*-benzypropyl] amino] benzophenone-glycine-Ni complex(43), and the camphor-derived Oppolzer's synthon(44) (Figure 8). These have in many cases afforded high *ee* syntheses of the desired L enantiomer. In addition, several chiral catalysts have been used including chiral diphosphine-rhodium(45) and more recently phase-transfer catalysts(46), applied to stereoselective hydrogenation and alkylation respectively.

An additional ^{11}C radiosynthetic challenge is the successful removal of potential reactants. In some cases these require special engineering solutions to remove reactive species. For example, use of ^{11}C-HCN is complicated by the presence of large quantities of NH_3. In the synthesis of [1-^{11}C] lactate via an acetaldehyde precursor, if NH_3 is not removed from the reaction milieu, the product is racemic [1-^{11}C] alanine(47). The possible reaction products are summarized in Figure 9. To synthesize [1-^{11}C] lactate, a trapping method was developed for ^{11}C-HCN consisting of NaOH applied to a platinum wire. This method successfully removed NH_3 from the reaction.

Studying the biochemistry of living systems

Basic energy metabolism- glycolysis and ketone bodies

As highlighted by the success of ^{18}F-FDG, the altered glycolysis seen in cancer and other diseases is a major target for imaging agent development. The majority of applications have been to human cancers. As reported in 1926 by Otto Warburg, tumors have altered metabolism, reverting to a primitive phenotype for energy. Warburg's studies found a remarkable preference of tumors for aerobic glycolysis over oxidative phosphorylation. This was a surprising result given the massive energy benefit complete oxidation of glucose confers. The "why" remains controversial, but the glycolytic phenotype seen in cancer has been leveraged in molecular imaging strategies. PET scans using ^{18}F-FDG are currently the standard of care for identifying tumors and detecting treatment response. Increasingly, ^{18}F-FDG is being used for other diseases including neurodegenerative disorders, seizures, inflammation, and infection.

Several metabolites involved in glycolysis have been ^{11}C labeled for metabolic study. One interesting feature of these ^{11}C molecules is the absence in many cases of a metabolic stopping point. A critical feature of ^{18}F-FDG is that substitution at the 2-position renders its phosphorylated adduct incapable of glucose-fructose isomerization by glucose-6-phosphate isomerase. This allows metabolic trapping of ^{18}F, and easier interpretation of PET-FDG data: retained tracer is a consequence of upregulated glucose (GLUT) transport and/or hexokinase activity in the tissues of interest. Interestingly, a similar strategy was used in the development of [2-^{11}C]-2-deoxyglucose as the ^{11}C counterpart for ^{18}F-FDG(48,49). In contrast, mechanistic trapping of most endogenous ^{11}C metabolites is not possible, although in several cases it is likely that the label is effectively trapped in a large steady-state pool. For example, aggressive tumors and their microenvironments have large steady-state concentrations of lactate. It is therefore likely that several ^{11}C substrates are converted to, and retained as ^{11}C lactate in these contexts. Similarly, many cell types in particular immune cells have high steady-state concentrations of Vitamin C. Therefore, if ^{11}C Vitamin C or ^{11}C dehydroascorbic acid is applied to inflamed tissues, it is likely that the retained label represents ^{11}C Vitamin C.

Numerous methods have been developed to label glucose, using ^{11}C cyanide(30), ^{11}C methylenetriphenylphosphorane(50), or nitromethane(51). Pyruvate has been prepared enzymatically from ^{11}C alanine(39), via ^{11}C cyanide or carboxylation of an acyl carbanion(52). Similarly, lactate has been generated enzymatically(39) or via ^{11}C cyanide(47). Acetate can enter glycolysis via acetyl coA and its ^{11}C version has been

synthesized via carboxylation of methyl-Grignard(53). ^{11}C glutamine, was synthesized recently from a chiral precursor using ^{11}C-CN(38), while [5-^{11}C] glutamate was obtained from *O*-acetyl-L-homoserine by enzymatic catalysis(54). Both of these metabolites can enter the TCA cycle via alpha-ketoglutarate, and glutaminolysis is upregulated in numerous human cancers(55). Finally, the role of alternate energy sources has been explored via the radiosynthesis of ^{11}C ketone bodies. In fasting, the normal brain increasingly relies on ketone bodies (β-hydroxybutyrate, acetoacetate, and acetone) produced in the liver from fatty acid β-oxidation. Both ^{11}C acetoacetate(56) and β-hydroxybutyrate have been synthesized, the latter via enzymatic conversion using β-hydroxybutyrate dehydrogenase(57).

DNA synthesis

Nucleoside analogs have a special role in antiviral therapeutics and nuclear imaging. The ^{18}F-thymidine analog ^{18}F-FLT has a mechanism similar to that of ^{18}F-FDG, whereby the probe is transported by ENT-1 and phosphorylated by thymidine kinase (TK)(58,59). [2-^{11}C] thymidine has been developed and tested as a PET tracer of thymidine incorporation into deoxyribonucleic acid (DNA), and thus as a means to detect cellular proliferation non-invasively. [2-^{11}C] thymidine is synthesized from [2-^{11}C] thymine, obtained by cyclization of ^{11}C urea and diethyl beta-methylmalate(60). After purification, [2-^{11}C] thymine and 2′-deoxyribose-1-phosphate are incubated in the presence of thymidine phosphorylase to form [2-^{11}C] thymidine. Another synthesis of ^{11}C thymidine using ^{11}C MeI has been reported(61). Although sophisticated modeling may be required, several authors have argued that the flux of [2-^{11}C] thymidine into DNA can serve as a marker of tumor proliferation(62).

Reduction and oxidation- Vitamin C and uric acid

The non-invasive detection of oxidative stress could have profound implications for the diagnosis and management of numerous diseases. Dysregulation of reactive oxygen species (ROS) provides a powerful motivation to develop non-invasive biomarkers of oxidative stress. A synthesis of ^{11}C Vitamin C was recently reported, synthesized from ^{11}C cyanide and L-xylosone based on a modification of the previously reported ^{13}C and ^{14}C enrichment techniques(27). The authors studied sensitivity to numerous inflammation-relevant ROS including H_2O_2, superoxide, and hypohlorite, and showed ROS-dependent accumulation in activated neutrophils. Another potential ROS-sensitive ^{11}C radiotracer synthesized recently is [^{11}C] uric acid. The synthesis of [^{11}C] uric acid was achieved by reacting 5,6-diaminouracil with ^{11}C phosgene(63). Uric acid has a well-known role in gout, but its known redox pairs (hypoxanthine and allantoin) have implicated it in numerous redox functions in vivo. One potential challenge in developing ROS-sensitive sensors for the noninvasive detection of oxidative stress is autoradiolysis(64). Studies of ^{11}C Vitamin C found that a high specific activity synthesis, while feasible, resulted in poor stability under physiologic conditions. It remains to be shown whether lower specific activity radiosynthesis, or other stabilizing strategies will afford sufficient sensitivity for *in vivo* ROS detection.

Metabolism of amino acids

Amino-acid derived PET tracers are applied frequently to study human cancers, especially brain tumors. The most important amino-acid derived radiotracer synthesized is ^{11}C L-methionine, which provided one of the first applications of ^{11}C methyl-iodide radiosynthesis(36). ^{11}C L-methionine studies in two patients with glioblastoma multiforme are shown in Figure 10(65). Since the use of ^{11}C L-methionine is restricted to PET centers with an on-site cyclotron and radiochemistry facility, promising results obtained with ^{11}C L-methionine have stimulated the development of ^{18}F-labelled aminoacid tracers, particularly O-(2-^{18}F-fluoeoethyl1)-L-tyrosine (FET)(66), ^{18}F-FACBC(67), and ^{18}F L-dopa(68). The latter has been used in oncologic applications in addition to Parkinson's disease. ^{11}C tyrosine has been used in human soft tissue sarcomas for which a protein synthesis rate was calculated(69).

Membranes, lipids and steroids

In ^{1}H magnetic resonance spectroscopy (^{1}H-MRS), choline as a component of cell membranes is interpreted as a marker for cellular membrane turnover. Elevations of choline as detected by ^{1}H-MRS are seen in neoplasms of both of the brain and prostate(70,71). An increased choline resonance on ^{1}H-MRS, as well as elevated uptake of ^{11}C choline are associated with increased cell proliferation and choline kinase activity. The most frequent synthesis of ^{11}C choline is via ^{11}C methyl-iodide, to generate [*N*-methyl-^{11}C] choline(72). Recently ^{18}F-choline has been used more frequently particularly in prostate cancer patients(73). Several fatty acids have been synthesized including ^{11}C arachidonic acid(74), an important signaling molecule and ^{11}C palmitate(75), synthesized via an ^{11}C alkyl iodide. The syntheses of endogenous steroids have been reported including [17α-^{11}C] methyltestosterone(76).

Neurotransmitters

Several neurotransmitters and their precursors have been studied including ^{11}C L-tyrosine(41), L-DOPA(77), L-tryptophan(31), 5-hydroxy-L-tryptophan(31), ^{11}C epinephrine(78) and ^{11}C norepinephrine(79). ^{11}C epinephrine has been used to study cardiac sympathetic nerve function in the context of heart transplantation, since the latter is associated with decreased sympathetic nerve integrity(80). An interesting study looking at cocaine toxicity showed that cocaine inhibited ^{11}C norepinephrine uptake in the heart, in monkeys(81).

Differential metabolism and site-specific ^{11}C labeling

One attractive feature of ^{11}C endogenous compounds is that they may be labeled at different nuclei, allowing the detection of divergent metabolism. An excellent example is ^{11}C pyruvate, which may be labeled at the 1 or 3-positions. In the heart, oxidative phosphorylation requires that pyruvate be decarboxylated to synthesize acetyl-CoA. When [1-^{11}C] pyruvate is decarboxylated, labeling of metabolically inert ^{11}C-CO_2 results in no tissue retention(35). In contrast, when [3-^{11}C] pyruvate is used the label is incorporated into

acetyl-CoA for import into mitochondria. An opposite result would be expected for the interrogation of highly glycolytic tumors. Specifically, reduced mitochondrial import of acetyl-CoA is typically seen in tumors, which are more likely to use aerobic glycolysis. ^{11}C pyruvate labeled at both the 1 and 3-positions would likely be incorporated into ^{11}C lactate and either retained in tumors or exported. Another excellent example of site-specific labeling used to identify the metabolic fate of nuclei was ^{11}C L-DOPA. L-DOPA may be labeled in either the β or carboxylic positions, with the label 'lost" as ^{11}C-CO_2 by the activity of DOPA-decarboxylase for the latter(82). Imaging studies using site-specific ^{11}C labeling to demonstrate decarboxylation are shown in Figure 11.

Endogenous ^{11}C tracers- synergy with other techniques

Recently, the study of endogenous ^{13}C nuclei *in vivo* has been enabled by a new spectroscopic imaging method, namely hyperpolarized (HP) ^{13}C MRS. This technique involves increasing the NMR-observable signal beyond that seen at thermal equilibrium, and has been applied to the study of several endogenous molecules including pyruvate, fumarate, bicarbonate, fructose, and ascorbic acid(83). The major advantage of this technique is direct observation of small molecules via their ^{13}C chemical shifts, allowing easy identification of metabolic products. In a typical experiment, enriched ^{13}C pyruvate is irradiated with microwave energy in a high magnetic field in the presence of a paramagnetic electron source, for approximately 1 hour at a temperature near absolute zero. After "polarization," the sample is rapidly heated, dissolved in aqueous solvent and injected intravenously. The real-time conversion of the introduced ^{13}C agent to various metabolites is then visualized via differences in chemical shift.

The most commonly employed hyperpolarized ^{13}C substrate is [1-^{13}C] pyruvic acid, which has been studied in a small cohort of prostate cancer patients(84), and in numerous preclinical oncology models. [1-^{13}C] pyruvate is converted rapidly to [1-^{13}C] lactate in numerous tumors, via the activity of NADH-dependent lactate dehydrogenase (LDH). The rate of this conversion has been shown to be grade-dependent in several tumor models(85). In these models, little or no ^{13}C CO_2 or ^{13}C HCO_3^- is visualized. In contrast, when [1-^{13}C] pyruvic acid is introduced into the myocardium of normal animals (for example pigs), rapid decarboxylation via PDH results in detection of a large ^{13}C HCO_3^- resonance. Absence of this signal may be a biomarker for myocardial ischemia and/or cardiac failure(86). Detection of these divergent pathways is analogous to what might be observed in similar biologic scenarios using ^{11}C pyruvate. In many cases data gleaned from ^{11}C PET and ^{13}C hyperpolarized MRI are complimentary, and elucidate the key mechanisms of image contrast. For example, development of the ^{13}C ascorbic acid/dehydroascorbic acid redox pair(87) for hyperpolarized MRI motivated the use of ^{11}C ascorbic acid as an endogenous redox sensor.

Acknowledgments

Acknowledgement of Grants: R01 CA 166766; T32 EB 001631

References

1. Maurer T, Eiber M, Schwaiger M, et al. Current use of PSMA-PET in prostate cancer management. Nat Rev Urol. 2016; 13:226–235. [PubMed: 26902337]
2. Rauscher I, Maurer T, Fendler WP, et al. (68)Ga-PSMA ligand PET/CT in patients with prostate cancer: How we review and report. Cancer Imaging. 2016; 16:14. [PubMed: 27277843]
3. Velikyan I. 68Ga-Based radiopharmaceuticals: production and application relationship. Molecules. 2015; 20:12913–12943. [PubMed: 26193247]
4. Mojtahedi A, Thamake S, Tworowska I, et al. The value of (68)Ga-DOTATATE PET/CT in diagnosis and management of neuroendocrine tumors compared to current FDA approved imaging modalities: a review of literature. Am J Nucl Med Mol Imaging. 2014; 4:426–434. [PubMed: 25143861]
5. Ariza M, Kolb HC, Moechars D, et al. Tau Positron Emission Tomography (PET) Imaging: Past, Present, and Future. J Med Chem. 2015; 58:4365–4382. [PubMed: 25671691]
6. Harada R, Okamura N, Furumoto S, et al. Characteristics of Tau and Its Ligands in PET Imaging. Biomolecules. 2016; 6:7. [PubMed: 26751494]
7. Vallabhajosula S. Positron emission tomography radiopharmaceuticals for imaging brain Beta-amyloid. Semin Nucl Med. 2011; 41:283–299. [PubMed: 21624562]
8. Yeo JM, Waddell B, Khan Z, et al. A systematic review and meta-analysis of (18)F-labeled amyloid imaging in Alzheimer's disease. Alzheimers Dement (Amst). 2015; 1:5–13. [PubMed: 27239488]
9. Klunk WE, Engler H, Nordberg A, et al. Imaging brain amyloid in Alzheimer's disease with Pittsburgh Compound-B. Ann Neurol. 2004; 55:306–319. [PubMed: 14991808]
10. Wong DF, Rosenberg PB, Zhou Y, et al. In vivo imaging of amyloid deposition in Alzheimer disease using the radioligand 18F-AV-45 (florbetapir [corrected] F 18). J Nucl Med. 2010; 51:913–920. [PubMed: 20501908]
11. Dannoon S, Ganguly T, Cahaya H, et al. Structure-Activity Relationship of (18)F-Labeled Phosphoramidate Peptidomimetic Prostate-Specific Membrane Antigen (PSMA)-Targeted Inhibitor Analogues for PET Imaging of Prostate Cancer. J Med Chem. 2016; 59:5684–5694. [PubMed: 27228467]
12. Masaki Y, Shimizu Y, Yoshioka T, et al. The accumulation mechanism of the hypoxia imaging probe "FMISO" by imaging mass spectrometry: possible involvement of low-molecular metabolites. Sci Rep. 2015; 5:16802. [PubMed: 26582591]
13. Narita T, Aoyama H, Hirata K, et al. Reoxygenation of glioblastoma multiforme treated with fractionated radiotherapy concomitant with temozolomide: changes defined by 18F-fluoromisonidazole positron emission tomography: two case reports. Jpn J Clin Oncol. 2012; 42:120–123. [PubMed: 22198964]
14. Fujibayashi Y, Taniuchi H, Yonekura Y, et al. Copper-62-ATSM: a new hypoxia imaging agent with high membrane permeability and low redox potential. J Nucl Med. 1997; 38:1155–1160. [PubMed: 9225812]
15. Flavell RR, Truillet C, Regan MK, et al. Caged [(18)F]FDG Glycosylamines for Imaging Acidic Tumor Microenvironments Using Positron Emission Tomography. Bioconjug Chem. 2016; 27:170–178. [PubMed: 26649808]
16. Carroll V, Michel BW, Blecha J, et al. A boronate-caged [(1)(8)F]FLT probe for hydrogen peroxide detection using positron emission tomography. J Am Chem Soc. 2014; 136:14742–14745. [PubMed: 25310369]
17. Liu W, Truillet C, Flavell RR, et al. A reactivity-based [F-18]FDG probe for in vivo formaldehyde imaging using positron emission tomography. Chemical Science. 2016; 7:5503–5507.
18. Lu C, Ward PS, Kapoor GS, et al. IDH mutation impairs histone demethylation and results in a block to cell differentiation. Nature. 2012; 483:474–U130. [PubMed: 22343901]
19. Ward PS, Cross JR, Lu C, et al. Identification of additional IDH mutations associated with oncometabolite R(−)-2-hydroxyglutarate production. Oncogene. 2012; 31:2491–2498. [PubMed: 21996744]
20. Dang L, White DW, Gross S, et al. Cancer-associated IDH1 mutations produce 2-hydroxyglutarate. Nature. 2009; 462:739–U752. [PubMed: 19935646]

21. Choi C, Ganji SK, DeBerardinis RJ, et al. 2-hydroxyglutarate detection by magnetic resonance spectroscopy in subjects with IDH-mutated gliomas. Nature Medicine. 2012; 18:624–629.
22. Elkhaled A, Jalbert LE, Phillips JJ, et al. Magnetic Resonance of 2-Hydroxyglutarate in IDH1-Mutated Low-Grade Gliomas. Science Translational Medicine. 2012; 4
23. Corpe CP, Lee JH, Kwon O, et al. 6-bromo-6-deoxy-L-ascorbic acid - An ascorbate analog specific for Na+-dependent vitamin C transporter but not glucose transporter pathways. Journal of Biological Chemistry. 2005; 280:5211–5220. [PubMed: 15590689]
24. Rumsey SC, Welch RW, Garraffo HM, et al. Specificity of ascorbate analogs for ascorbate transport - Synthesis and detection of [I-125]-6-deoxy-6-iodo-1-ascorbic acid and characterization of its ascorbate-specific transport properties. Journal of Biological Chemistry. 1999; 274:23215–23222. [PubMed: 10438494]
25. Yamamoto F, Sasaki S, Maeda M. Positron Labeled Antioxidants - Synthesis and Tissue Biodistribution of 6-Deoxy-6-[F-18]Fluoro-L-Ascorbic Acid. Applied Radiation and Isotopes. 1992; 43:633–639. [PubMed: 1325422]
26. Kothari PJ, Finn RD, Bornmann WG, et al. Chemical consequences resulting from multi-millicurie preparation of 6-[F-18]-fluoro-6-deoxy-L-ascorbic acid. Radiochimica Acta. 1997; 77:87–90.
27. Carroll VN, Truillet C, Shen B, et al. [(11)C]Ascorbic and [(11)C]dehydroascorbic acid, an endogenous redox pair for sensing reactive oxygen species using positron emission tomography. Chem Commun (Camb). 2016; 52:4888–4890. [PubMed: 26963495]
28. Hartvig P, Lindner KJ, Tedroff J, et al. Regional Brain Kinetics of 6-Fluoro-(Beta-11c)-L-Dopa and Beta-11c)-L-Dopa Following Comt Inhibition - a Study Invivo Using Positron Emission Tomography. Journal of Neural Transmission-General Section. 1992; 87:15–22. [PubMed: 1536715]
29. Straatmann M, Welch MJ. Liquid Chromatographic Purification of Carbon-11 Labeled Glucose. International Journal of Applied Radiation and Isotopes. 1973; 24:234–236. [PubMed: 4696811]
30. Shiue CY, Wolf AP. The Syntheses of L-[C-11]-D-Glucose and Related-Compounds for the Measurement of Brain Glucose-Metabolism. Journal of Labelled Compounds & Radiopharmaceuticals. 1985; 22:171–182.
31. Bjurling P, Antoni G, Watanabe Y, et al. Enzymatic-Synthesis of Carboxy-C-11-Labeled L-Tyrosine, L-Dopa, L-Tryptophan and 5-Hydroxy-L-Tryptophan. Acta Chemica Scandinavica. 1990; 44:178–182.
32. Scott PJ. Methods for the incorporation of carbon-11 to generate radiopharmaceuticals for PET imaging. Angew Chem Int Ed Engl. 2009; 48:6001–6004. [PubMed: 19554578]
33. Langstrom B, Karimi F, Watanabe Y. Endogenous compounds labeled with radionuclides of short half-life-some perspectives. J Labelled Comp Radiopharm. 2013; 56:251–262. [PubMed: 24285332]
34. Miller PW, Long NJ, Vilar R, et al. Synthesis of 11C, 18F, 15O, and 13N radiolabels for positron emission tomography. Angew Chem Int Ed Engl. 2008; 47:8998–9033. [PubMed: 18988199]
35. Antoni G. Development of carbon-11 labelled PET tracers-radiochemical and technological challenges in a historic perspective. J Labelled Comp Radiopharm. 2015; 58:65–72. [PubMed: 25684179]
36. Langstrom B, Antoni G, Gullberg P, et al. Synthesis of L- and D-[methyl-11C]methionine. J Nucl Med. 1987; 28:1037–1040. [PubMed: 3585494]
37. Gomzina NA, Kuznetsova OF. L-[methyl-(11C)]-methionine of high enantiomeric purity production via on-line 11C-methylation of L-homocysteine thiolactone hydrochloride. Bioorg Khim. 2011; 37:216–222. [PubMed: 21721254]
38. Qu W, Oya S, Lieberman BP, et al. Preparation and characterization of L-[5-11C]-glutamine for metabolic imaging of tumors. J Nucl Med. 2012; 53:98–105. [PubMed: 22173839]
39. Ropchan JR, Barrio JR. Enzymatic-Synthesis of [1-C-11] Pyruvic-Acid, L-[1-C-11]Lactic Acid and L-[1-C-11]Alanine Via Dl-[1-C-11]Alanine. Journal of Nuclear Medicine. 1984; 25:887–892. [PubMed: 6611389]
40. Barrio JR, Keen RE, Ropchan JR, et al. L-(1-C-11)leucine - Routine Synthesis by Enzymatic Resolution. Journal of Nuclear Medicine. 1983; 24:515–521. [PubMed: 6602211]

41. Halldin C, Schoeps KO, Stoneelander S, et al. The Bucherer-Strecker Synthesis of D-(1-C-11)Tyrosine and L-(1-C-11)Tyrosine and the Invivo Study of L-(1-C-11)Tyrosine in Human-Brain Using Positron Emission Tomography. European Journal of Nuclear Medicine. 1987; 13:288–291. [PubMed: 3499325]
42. Antoni G, Fasth KJ, Malmborg P, et al. Synthesis of Dl- and L-[3-C-11]-Amino Acids. Journal of Labelled Compounds & Radiopharmaceuticals. 1986; 23:1056–1058.
43. Fasth KJ, Antoni G, Malmborg P, et al. Asymmetric-Synthesis of C-11-Labelled Amino-Acids. Applied Radiation and Isotopes. 1988; 39:581–581.
44. Oppolzer W, Moretti R, Zhou CY. Asymmetric Alkylations of a Sultam-Derived Glycine Equivalent - Practical Preparation of Enantiomerically Pure Alpha-Amino-Acids. Helvetica Chimica Acta. 1994; 77:2363–2380.
45. Halldin C, Langstrom B. Asymmetric-Synthesis of 3-C-11] L-Phenylalanine Using Chiral Hydrogenation Catalysts. International Journal of Applied Radiation and Isotopes. 1984; 35:945–948.
46. Filp U, Pekosak A, Poot AJ, et al. Enantioselective synthesis of carbon-11 labeled L-alanine using phase transfer catalysis of Schiff bases. Tetrahedron. 2016; 72:6551–6557.
47. Drandarov K, Schubiger PA, Westera G. Automated no-carrier-added synthesis of [1-C-11]-labeled D- and L-enantiomers of lactic acid. Applied Radiation and Isotopes. 2006; 64:1613–1622. [PubMed: 16854588]
48. Volkow ND, Brodie JD, Wolf AP, et al. Brain Metabolism in Patients with Schizophrenia before and after Acute Neuroleptic Administration. Journal of Neurology Neurosurgery and Psychiatry. 1986; 49:1199–1202.
49. Stoneelander S, Nilsson JLG, Blomqvist G, et al. C-11-2-Deoxy-D-Glucose - Synthesis and Preliminary Comparison with C-11-D-Glucose as a Tracer for Cerebral Energy-Metabolism in Pet Studies. European Journal of Nuclear Medicine. 1985; 10:481–486. [PubMed: 3875488]
50. Grierson JR, Biskupiak JE, Link JM, et al. Radiosynthesis of 6-[C-11]-D-Glucose. Applied Radiation and Isotopes. 1993; 44:1449–1458. [PubMed: 8257963]
51. Schoeps KO, Langstrom B, Stoneelander S, et al. Synthesis of (1-C-11)D-Glucose and (1-C-11)D-Mannose from Online Produced (C-11)Nitromethane. Applied Radiation and Isotopes. 1991; 42:877–883. [PubMed: 1657835]
52. Kilbourn MR, Welch MJ. No-Carrier-Added Synthesis of [1-C-11-Labeled Pyruvic-Acid. International Journal of Applied Radiation and Isotopes. 1982; 33:359–361. [PubMed: 7095876]
53. Le Bars D, Malleval M, Bonnefoi F, et al. Simple synthesis of [1-C-11]acetate. Journal of Labelled Compounds & Radiopharmaceuticals. 2006; 49:263–267.
54. Antoni G, Omura H, Ikemoto M, et al. Enzyme catalysed synthesis of L-[4-C-11]aspartate and L-[5-C-11]glutamate. Journal of Labelled Compounds & Radiopharmaceuticals. 2001; 44:287–294.
55. Altman BJ, Stine ZE, Dang CV. From Krebs to clinic: glutamine metabolism to cancer therapy. Nat Rev Cancer. 2016; 16:619–634. [PubMed: 27492215]
56. Straatmann MG, Hortmann AG, Welch MJ. Preparation of C-11-Labeled Acetoacetic Acid. Journal of Nuclear Medicine. 1973; 14:457–458.
57. Tremblay S, Ouellet R, Benard F, et al. Automated synthesis of C-11-beta-hydroxybutyrate by enzymatic conversion of C-11-acetoacetate using beta-hydroxybutyrate dehydrogenase. Journal of Labelled Compounds & Radiopharmaceuticals. 2008; 51:242–245.
58. Brockenbrough JS, Souquet T, Morihara JK, et al. Tumor 3′-deoxy-3′-(18)F-fluorothymidine ((18)F-FLT) uptake by PET correlates with thymidine kinase 1 expression: static and kinetic analysis of (18)F-FLT PET studies in lung tumors. J Nucl Med. 2011; 52:1181–1188. [PubMed: 21764789]
59. Paproski RJ, Wuest M, Jans HS, et al. Biodistribution and uptake of 3′-deoxy-3′-fluorothymidine in ENT1-knockout mice and in an ENT1-knockdown tumor model. J Nucl Med. 2010; 51:1447–1455. [PubMed: 20720035]
60. Vanderborght T, Labar D, Pauwels S, et al. Production of [2-C-11]Thymidine for Quantification of Cellular Proliferation with Pet. Applied Radiation and Isotopes. 1991; 42:103–104. [PubMed: 1850393]

61. Poupeye E, Counsell RE, Deleenheer A, et al. Synthesis of C-11-Labelled Thymidine for Tumor Visualization Using Positron Emission Tomography. Applied Radiation and Isotopes. 1989; 40:57–61. [PubMed: 2540122]
62. Mankoff DA, Shields AF, Link JM, et al. Kinetic analysis of 2-[11C]thymidine PET imaging studies: validation studies. J Nucl Med. 1999; 40:614–624. [PubMed: 10210220]
63. Yashio K, Katayama Y, Takashima T, et al. Synthesis of [(1)(1)C]uric acid, using [(1)(1)C]phosgene, as a possible biomarker in PET imaging for diagnosis of gout. Bioorg Med Chem Lett. 2012; 22:115–119. [PubMed: 22153940]
64. Scott PJ, Hockley BG, Kung HF, et al. Studies into radiolytic decomposition of fluorine-18 labeled radiopharmaceuticals for positron emission tomography. Appl Radiat Isot. 2009; 67:88–94. [PubMed: 18951032]
65. Terakawa Y, Tsuyuguchi N, Iwai Y, et al. Diagnostic accuracy of 11C-methionine PET for differentiation of recurrent brain tumors from radiation necrosis after radiotherapy. J Nucl Med. 2008; 49:694–699. [PubMed: 18413375]
66. Dunet V, Rossier C, Buck A, et al. Performance of 18F-fluoro-ethyl-tyrosine (18F-FET) PET for the differential diagnosis of primary brain tumor: a systematic review and Metaanalysis. J Nucl Med. 2012; 53:207–214. [PubMed: 22302961]
67. Shoup TM, Olson J, Hoffman JM, et al. Synthesis and evaluation of [18F]1-amino-3-fluorocyclobutane-1-carboxylic acid to image brain tumors. J Nucl Med. 1999; 40:331–338. [PubMed: 10025843]
68. Heiss WD, Wienhard K, Wagner R, et al. F-Dopa as an amino acid tracer to detect brain tumors. J Nucl Med. 1996; 37:1180–1182. [PubMed: 8965194]
69. Plaat B, Kole A, Mastik M, et al. Protein synthesis rate measured with L-[1-11C]tyrosine positron emission tomography correlates with mitotic activity and MIB-1 antibody-detected proliferation in human soft tissue sarcomas. Eur J Nucl Med. 1999; 26:328–332. [PubMed: 10199937]
70. Kurhanewicz J, Vigneron DB. Advances in MR spectroscopy of the prostate. Magn Reson Imaging Clin N Am. 2008; 16:697–710. ix–x. [PubMed: 18926432]
71. Wang W, Hu Y, Lu P, et al. Evaluation of the diagnostic performance of magnetic resonance spectroscopy in brain tumors: a systematic review and meta-analysis. PLoS One. 2014; 9:e112577. [PubMed: 25393009]
72. Diksic M, Yamamoto YL, Feindel W. Synthesis of C-11-Labelled Choline. Journal of Labelled Compounds & Radiopharmaceuticals. 1984; 21:815–820.
73. DeGrado TR, Coleman RE, Wang SY, et al. Synthesis and evaluation of F-18-labeled choline as an oncologic tracer for positron emission tomography: Initial findings in prostate cancer. Cancer Research. 2001; 61:110–117. [PubMed: 11196147]
74. Kihlberg T, Langstrom B. Synthesis of [19-C-11]Arachidonic Acid. Journal of Labelled Compounds & Radiopharmaceuticals. 1994; 34:617–626.
75. Buckman BO, Vanbrocklin HF, Dence CS, et al. Synthesis and Tissue Biodistribution of [Omega-C-11]Palmitic Acid - a Novel Pet Imaging Agent for Cardiac Fatty-Acid Metabolism. Journal of Medicinal Chemistry. 1994; 37:2481–2485. [PubMed: 8057294]
76. Berger G, Maziere M, Prenant C, et al. Synthesis of High Specific Activity C-11 17-Alpha Methyltestosterone. International Journal of Applied Radiation and Isotopes. 1981; 32:811–815. [PubMed: 7309270]
77. Bolster JM, Vaalburg W, Van Veen W, et al. Synthesis of no-carrier-added L- and D-[1-11C]-DOPA. Int J Appl Radiat Isot. 1983; 34:1650–1652. [PubMed: 6421752]
78. Chakraborty PK, Gildersleeve DL, Jewett DM, et al. High-Yield Synthesis of High Specific Activity R-(−)-[C-11]Epinephrine for Routine Pet Studies in Humans. Nuclear Medicine and Biology. 1993; 20:939–944. [PubMed: 8298573]
79. Nagren K, Schoeps KO, Halldin C, et al. Selective Synthesis of Racemic 1-C-11-Labeled Norepinephrine, Octopamine, Norphenylephrine and Phenylethanolamine Using [C-11]Nitromethane. Applied Radiation and Isotopes. 1994; 45:515–521. [PubMed: 8186772]
80. Munch G, Nguyen NTB, Nekolla S, et al. Evaluation of sympathetic nerve terminals with [C-11]epinephrine and [C-11]hydroxyephedrine and positron emission tomography. Circulation. 2000; 101:516–523. [PubMed: 10662749]

81. Suhara T, Farde L, Halldin C, et al. Effects of cocaine on [11C]norepinephrine and [11C] beta-CIT uptake in the primate peripheral organs measured by PET. Ann Nucl Med. 1996; 10:85–88. [PubMed: 8814732]

82. Bergstrom M, Eriksson B, Oberg K, et al. In vivo demonstration of enzyme activity in endocrine pancreatic tumors: Decarboxylation of carbon-11-DOPA to carbon-11-dopamine. Journal of Nuclear Medicine. 1996; 37:32–37. [PubMed: 8543997]

83. Keshari KR, Wilson DM. Chemistry and biochemistry of C-13 hyperpolarized magnetic resonance using dynamic nuclear polarization. Chemical Society Reviews. 2014; 43:1627–1659. [PubMed: 24363044]

84. Nelson SJ, Kurhanewicz J, Vigneron DB, et al. Metabolic Imaging of Patients with Prostate Cancer Using Hyperpolarized [1-C-13]Pyruvate. Science Translational Medicine. 2013; 5

85. Albers MJ, Bok R, Chen AP, et al. Hyperpolarized C-13 Lactate, Pyruvate, and Alanine: Noninvasive Biomarkers for Prostate Cancer Detection and Grading. Cancer Research. 2008; 68:8607–8615. [PubMed: 18922937]

86. Schroeder MA, Lau AZ, Chen AP, et al. Hyperpolarized C-13 magnetic resonance reveals early- and late-onset changes to in vivo pyruvate metabolism in the failing heart. European Journal of Heart Failure. 2013; 15:130–140. [PubMed: 23258802]

87. Keshari KR, Kurhanewicz J, Bok R, et al. Hyperpolarized C-13 dehydroascorbate as an endogenous redox sensor for in vivo metabolic imaging. Proceedings of the National Academy of Sciences of the United States of America. 2011; 108:18606–18611. [PubMed: 22042839]

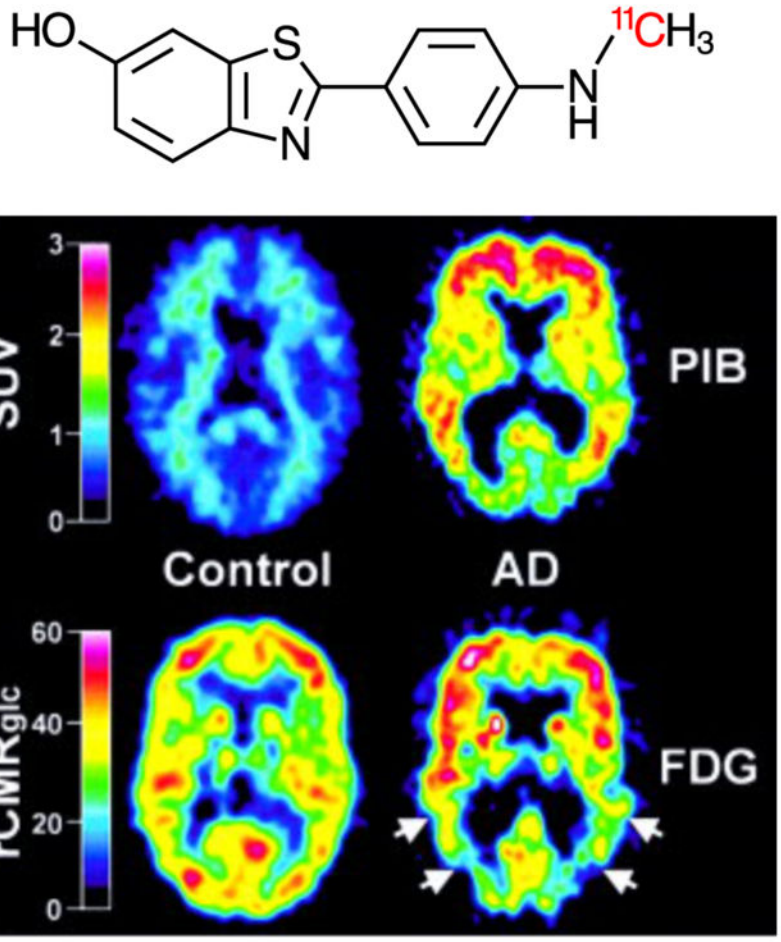

Figure 1.

Affinity-based tracer Pittsburgh compound B (PiB), an ^{11}C analog of thioflavin T. This compound is used to image β-amyloid plaques seen in neurodegenerative diseases including Alzheimers. In this case the tracer showed markedly increased uptake in the brain of an Alzheimers patient relative to a healthy control. An ^{18}F FDG is shown for comparison showing areas of hypometabolism. Figure adapted from Klunk *et al.* 2004.

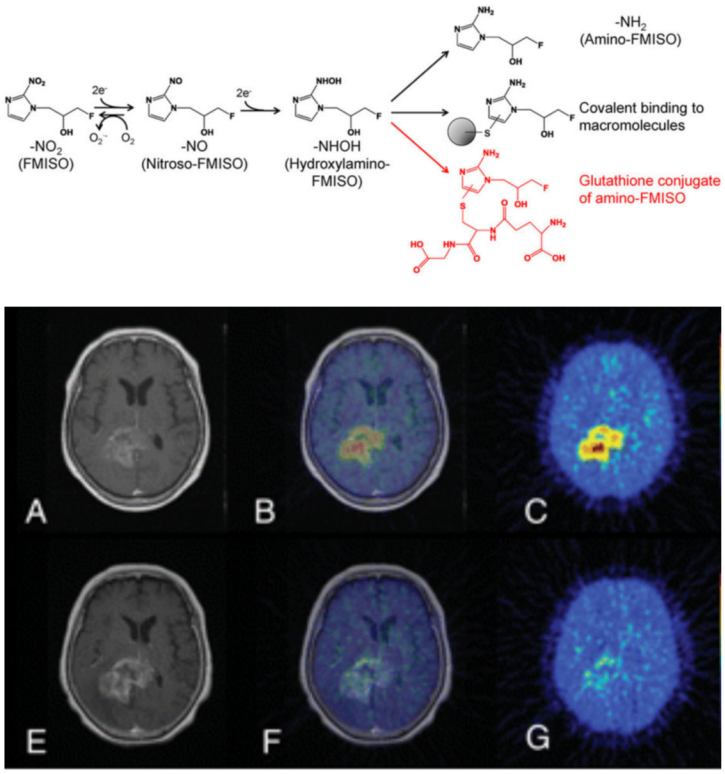

Figure 2.

Putative mechanism of ^{18}F-FMISO accumulation. In hypoxic tissues sequential reduction of ^{18}F-FMISO results in a species capable of both covalent binding to macromolecules and conjugation to reduced glutathione (GSH). The lower images show dramatic effects of tumor reoxygenation after radiation therapy in glioblastoma multiforme. Images A through C show images from a patient before therapy (C shows an ^{18}F-FMISO-PET image). E through G show images following therapy, demonstrating marked decrease in ^{18}F-FMISO retention despite a similar MRI appearance. Figure adapted from *Masaki et al.* 2016 and Narita *et al.* 2012.

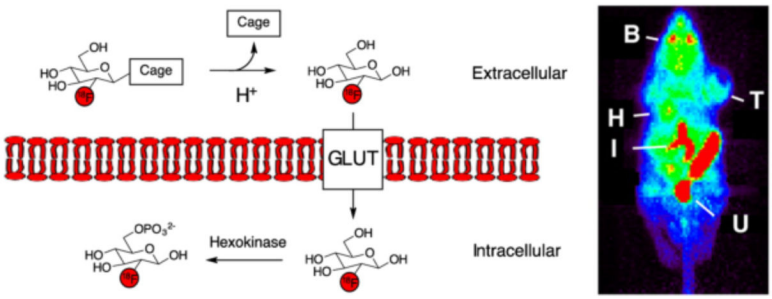

Figure 3.

Analyte-sensing strategy using an ^{18}F-FDG precursor. In this case the FDG precursor is labile at acidic pH, promoting decomposition to ^{18}F-FDG in the tumoral microenvironment. In preclinical imaging studies, high tumor uptake was seen while brain activity was suppressed. Adapted from Flavell *et al.* 2016.

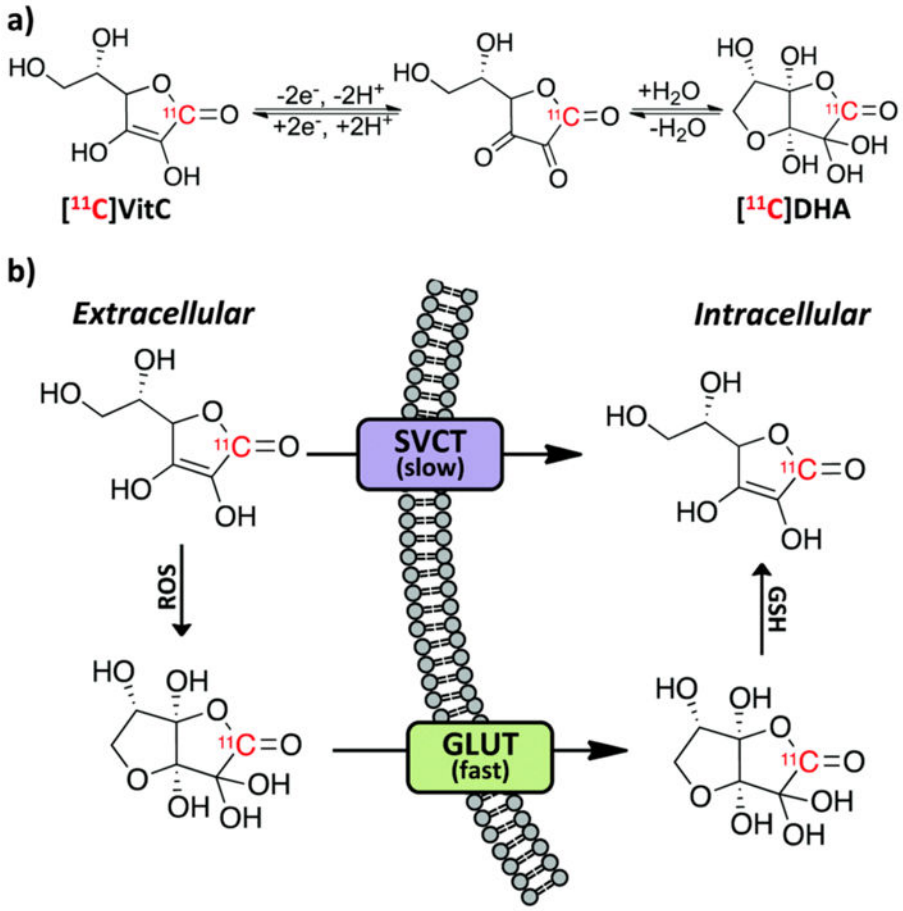

Figure 4.

Oxidation of [1-^{11}C] Vitamin C. (A) Two-electron oxidation of Vitamin C to dehydroascorbic acid (DHA) results in a species that exists in solution as a bicyclic hemiketal. Cyclization requires a 6-OH and this form is believed to be responsible for GLUT-mediated uptake. (B) Mechanism of [1-^{11}C] Vitamin C reactive oxygen species (ROS) sensing. Adapted from Carroll *et al.* 2016.

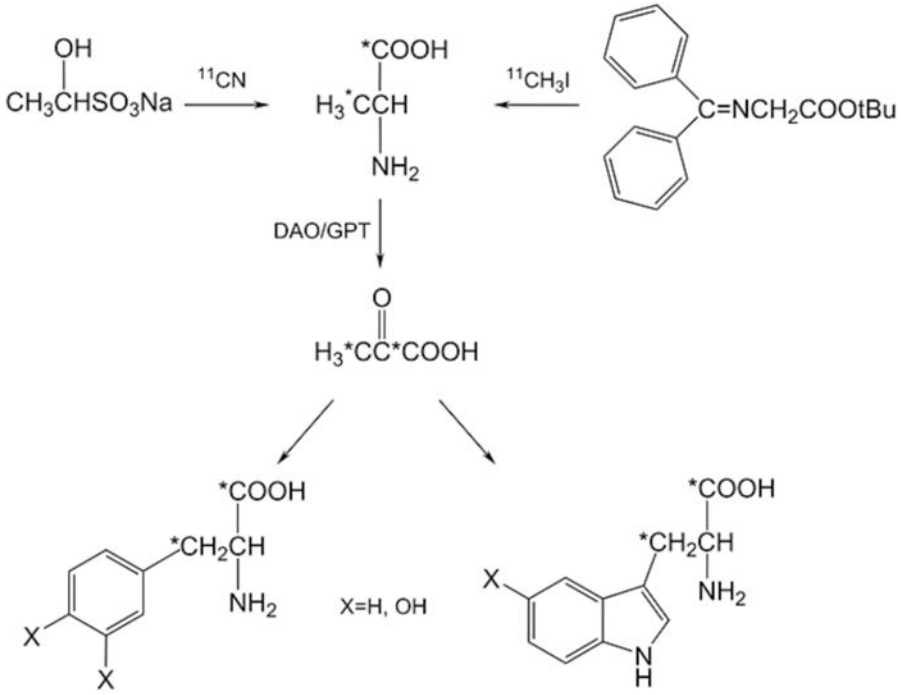

Figure 5.

Synthesis of ^{11}C tyrosine and ^{11}C tryptophan via a single-pot enzymatic synthesis. Purification of the L-isomer was made possible by use of D-amino acid oxidase. Adapted from Antoni *et al.* 2015.

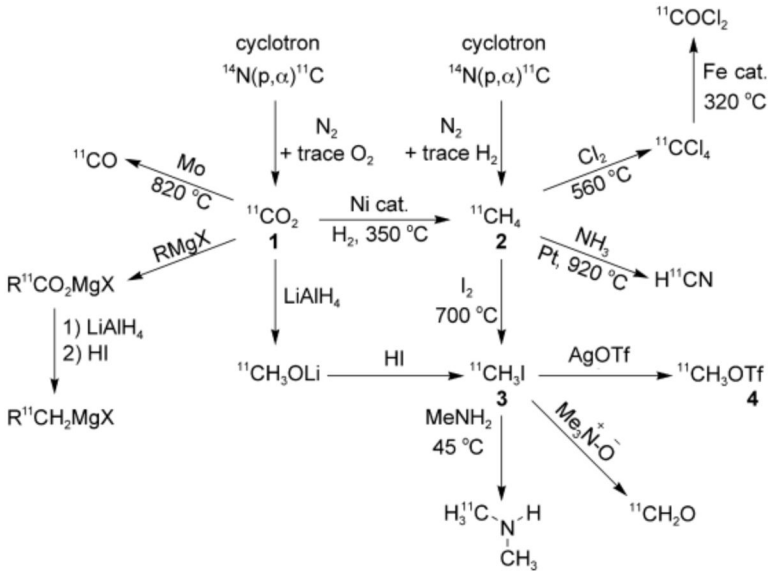

Figure 6.
Common building blocks in ^{11}C radiochemical synthesis. Adapted from Scott 2009.

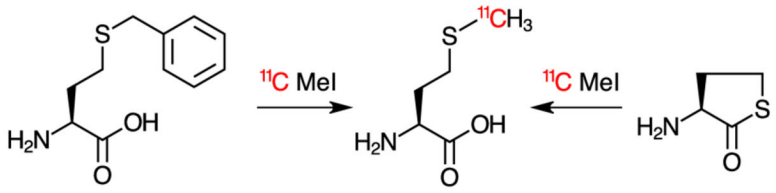

Figure 7.
Syntheses of ^{11}C L-methionine.

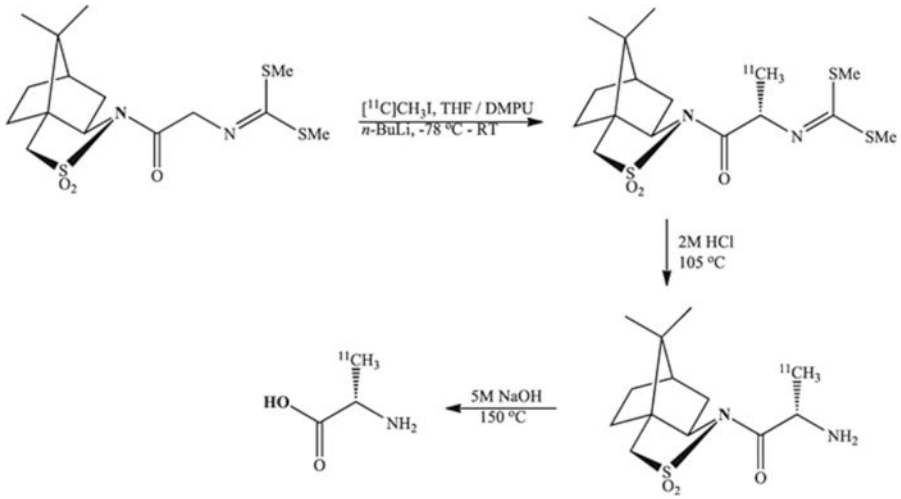

Figure 8.

Radiosynthesis of [3-^{11}C] L-alanine via an Oppolzer's synthon-derived glycine equivalent. Adapted from Langstrom *et al.* 2013.

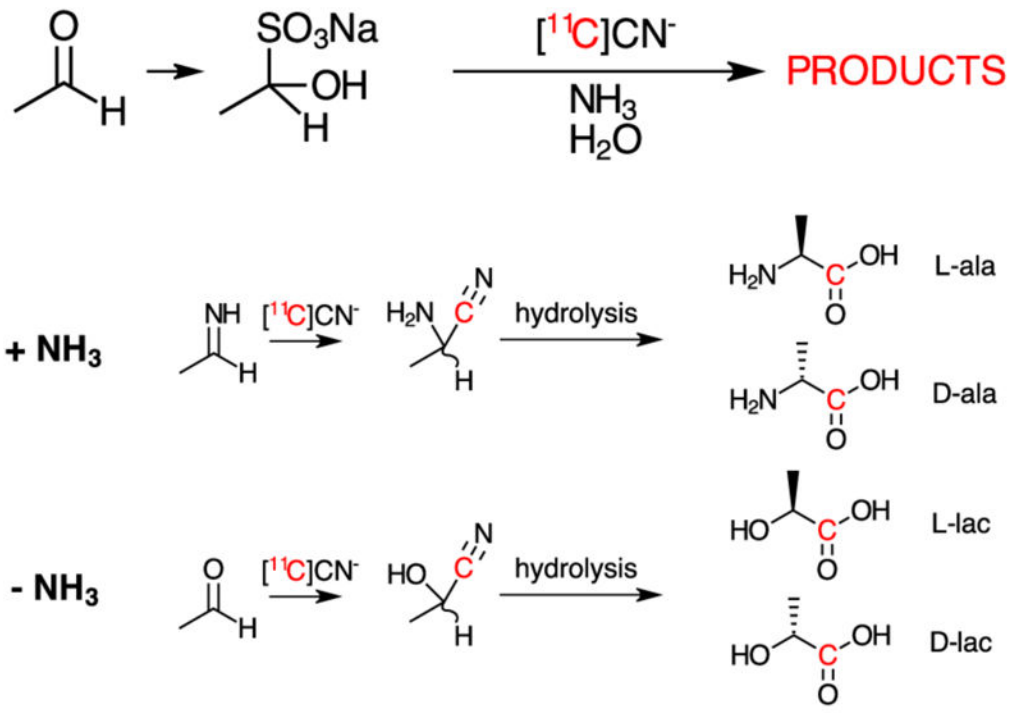

Figure 9.
Synthesis of [1-^{11}C] lactate via ^{11}C-cyanide depends on the successful scavenging of NH_3.

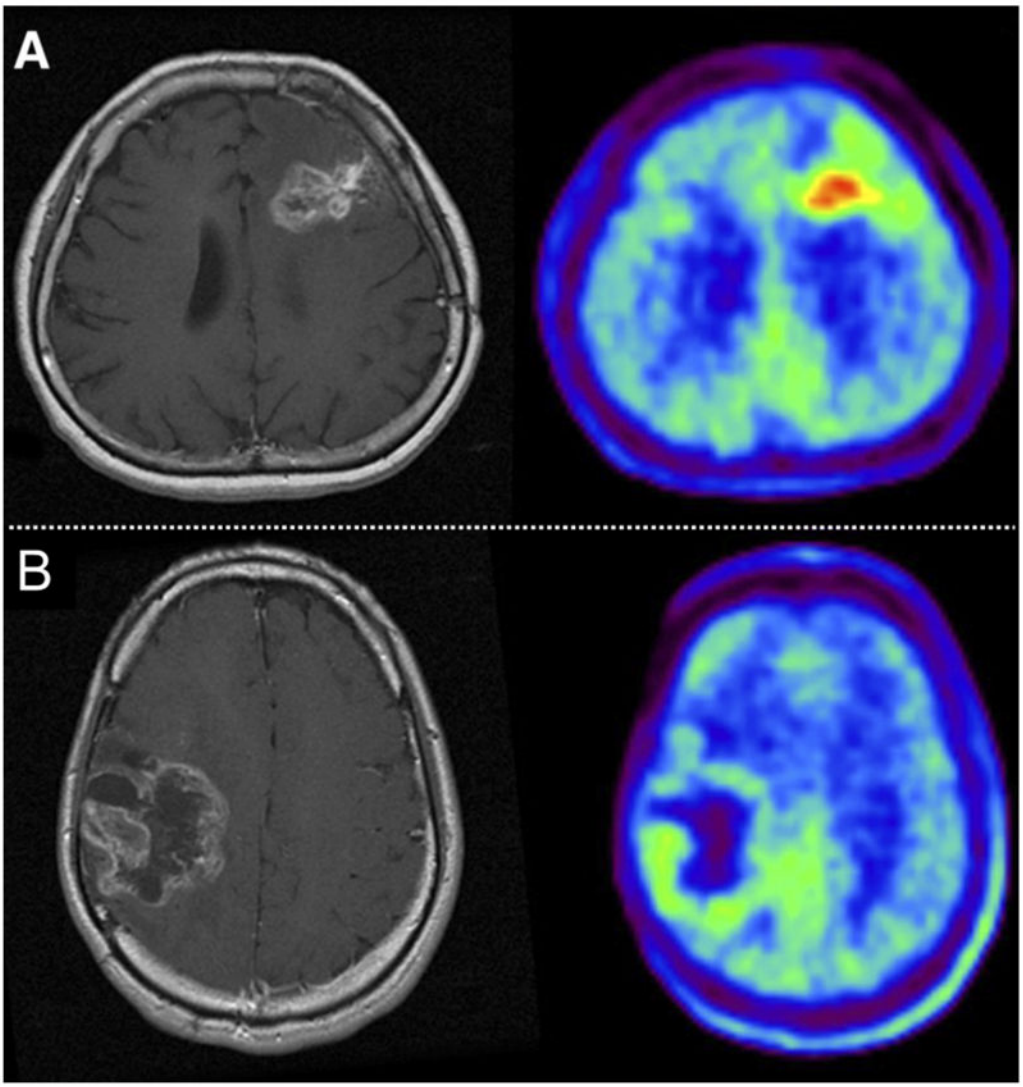

Figure 10.

Brain tumor studies using ^{11}C L-methionine. In some cases this tracer allows distinction between recurrent tumor (A, pathologically proven) and radiation necrosis (B). Adapted from Terakawa *et al.* 2008.

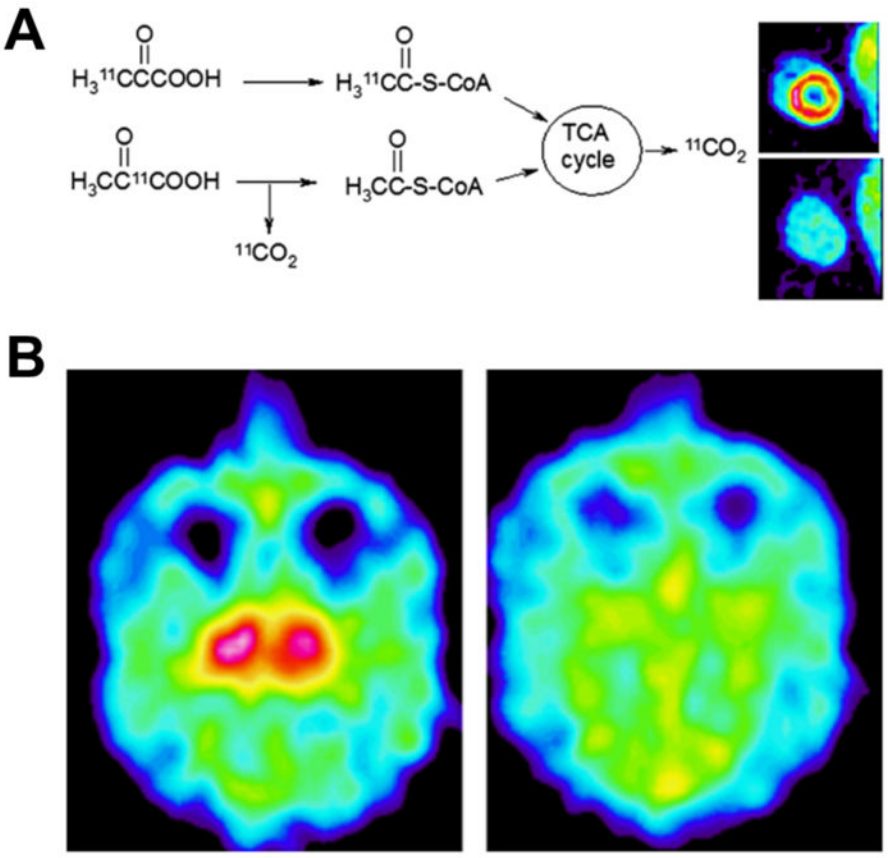

Figure 11.

Site-specific labeling of ^{11}C probes allows detection of differential metabolism. (A) Incorporation of ^{11}C into the myocardium is seen with [3-^{11}C] pyruvate, since the label is transferred to acetyl-CoA which enters the TCA cycle. In contrast the label is "lost" following decarboxylation for [1-^{11}C] pyruvate. (B) Similar findings with [1-^{11}C] L-dope, with loss of the label as ^{11}C CO_2. Adapted from Antoni *et al.* 2015.